Acta Astronautica 116 (2015) 43–49

Contents lists available at ScienceDirect

Acta Astronautica

journal homepage: www.elsevier.com/locate/actaastro

Electric solar wind sail optimal transit in the circular restricted three body problem

Alessandro A. Quarta*, Generoso Aliasi, Giovanni Mengali

Department of Civil and Industrial Engineering, University of Pisa, I-56122 Pisa, Italy

ARTICLE INFO

Article history:
Received 19 December 2014
Received in revised form
10 April 2015
Accepted 21 June 2015
Available online 29 June 2015

Keywords:
Electric solar wind sail
Artificial equilibrium point
Lagrangian points tour

ABSTRACT

This paper analyzes the transfer orbits within a Sun−[Earth+Moon] system for a spacecraft whose primary propulsion system is an Electric Solar Wind Sail. The planetary system is approximated through the Circular Restricted Three Body Problem and the spacecraft motion is studied in an optimal framework in which the performance index is the flight time. Minimum time transfers are studied using an indirect approach, and the optimal control law is found in analytical form as a function of the problem parameters. Optimal transfers between equilibrium points are discussed and interesting symmetries in the spacecraft trajectories are pointed out along with an analytical proof of their existence. A mission scenario consistent with the Geostorm concept is analyzed and the effectiveness of the propulsion system is emphasized for missions involving a tour through a subset of the classical Lagrangian points.

© 2015 IAA. Published by Elsevier Ltd. All rights reserved.

1. Introduction

The Electric Solar Wind Sail (E-sail) is an innovative form of spacecraft propulsion system that exploits the solar wind plasma momentum by repelling positive ions using a number of long tethers biased at a high positive voltage [1–3]. Similar to other continuous thrust propulsion systems, an E-sail enables a wide range of new mission concepts [4] such as, for example, the generation of Artificial Equilibrium Points (AEPs) within an heliocentric mission scenario. An AEP may be thought of as a special case of a spacecraft motion within a Circular Restricted Three Body Problem (CRTBP). The dynamics of a massless point in the CRTBP is a classical mathematical model [5] that is usually adopted to approximate the spacecraft motion within the Earth–Moon system or the Sun–[Earth+Moon] system [6–8].

A thorough analysis of mission applications involving AEPs has been addressed in recent years. In particular, different studies regarding the use of solar sails [9], E-sails [10,11], and electric thrusters [12] have shown the existence of infinite equilibrium surfaces in the CRTBP. The shape of those surfaces depends on both the physical characteristics of the celestial bodies involved in the problem and the spacecraft propulsive capabilities, in terms of maximum propulsive acceleration and technological constraints associated to the thrust direction.

In a typical mission scenario involving the use of an AEP, the spacecraft is required to exploit the propulsion system acceleration to reach and maintain one point of the equilibrium surfaces over a sufficiently long time period [13]. However, the availability of a continuous thrust also allows the spacecraft to be moved among different targets within the set of accessible equilibrium points. This capability makes the mission more flexible, as different mission objectives can be reached using a single spacecraft in a sufficiently large time interval. In this context, another interesting possibility is to initially release multiple spacecraft at the same AEP, and

* Corresponding author.
E-mail addresses: a.quarta@ing.unipi.it (A.A. Quarta), gen.aliasi@gmail.com (G. Aliasi), g.mengali@ing.unipi.it (G. Mengali).

http://dx.doi.org/10.1016/j.actaastro.2015.06.017
0094-5765/© 2015 IAA. Published by Elsevier Ltd. All rights reserved.

Nomenclature

$\mathbf{a}_P$	propulsive acceleration vector
a_c	spacecraft characteristic acceleration
C	system's center-of-mass
G	universal gravitational constant
$\hat{\mathbf{i}}$, $\hat{\mathbf{j}}$, $\hat{\mathbf{k}}$	unit vectors of the synodic frame
J	performance index
l	Sun−[Earth+Moon] distance (with $l=1$ au)
m	mass
$\mathbb{E}$	auxiliary matrix, see Eq. (9)
$\mathbf{r}$	dimensionless spacecraft position vector (w.r.t. C)
t	time
$\mathbf{v}$	dimensionless velocity (derivative of $\mathbf{r}$ w.r.t. ν)
α	cone angle
β	lightness number
$\boldsymbol{\lambda}_s$	vector adjoint to variable $\mathbf{s}$
μ	dimensionless mass
ν	angular variable
$\boldsymbol{\rho}$	dimensionless celestial body-spacecraft vector (with $\rho=\Vert\boldsymbol{\rho}\Vert$)
τ	switching parameter

Subscripts

0	artificial equilibrium point
f	final
gs	Geostorm mission case
i	initial
L_j	classical Lagrangian point (with $j=1\ldots5$)
max	maximum
$\oplus$	Earth+Moon
$\odot$	Sun

Superscripts

$'$	derivative w.r.t. ν
$\wedge$	unit vector
$\sim$	depending on the controls

then displace each spacecraft at different pre-selected AEP locations, similar to what is required by the L_1-Diamond mission concept proposed by Sauer [14] about 10 years ago. More recent studies [15,16], exploring potential and innovative applications of solar sails, have started to investigate also the transfer between a given set of AEPs by inspecting, for example, the linear dynamics of the spacecraft around its equilibrium point.

This paper analyzes the time-optimal transfer between equilibrium points within the Sun–[Earth+Moon] system for an E-sail based spacecraft. Within this context, the new contribution is to develop a mathematical model where, using an indirect approach, the optimal control law is obtained in an analytical form as a function of the state variables involved in the problem. The control law is then applied for simulating minimum time trajectories and investigating the E-sail performance. In particular, two different mission scenarios are discussed in detail. The first one, which is consistent with the Geostorm mission concept [13], concerns the optimal transfer between the classical L_1 point and a collinear AEP (that is, a point along the segment between Sun and Earth+Moon). The second mission example refers to a tour through a subset of the classical Lagrangian points. The problem considered is to find the minimum transfer time, for all of the pairs of points within the set, using an E-sail based spacecraft with a given (canonical) characteristic acceleration.

The results discussed in this paper are part of an European research project [3,17,18] regarding the study and development of an E-sail thruster, and are intended to contribute to the definition of the set of possible scenarios [4] within which a selection is to be made for testing the practical feasibility of the propulsion system in a real mission. For this reason no performance comparison is made here with other propellantless thrusters, such as solar sails, nor with other low-thrust propulsion systems, as, for example, electric thrusters. As a matter of fact such a comparison would imply an analysis of the spacecraft mass budget, which is however well beyond the scope of this work.

The paper is organized as follows. The first section illustrates the mathematical model used for the study of spacecraft dynamics in the CRTBP and for the calculation of the optimal trajectory. It also includes a detailed discussion of the steering law, how it has been obtained with an indirect approach and the definition of the Two-Point Boundary Value Problem (TPBVP) associated to the optimization problem. The methodology used to solve the TPBVP is only briefly summarized as the numerical techniques are well known. Section 3 involves the application of the mathematical model to the two mission scenarios that have been described above. This section also contains an analysis of the symmetric structure arising from the optimal trajectory. Such a symmetry finds a practical application in the solution of the TPBVP. Some final remarks conclude, as usual, the paper.

2. Mathematical model

The motion of the E-sail-based spacecraft is governed by the gravitational field of the two massive bodies (i.e., the Sun of mass $m_\odot$ and the Earth+Moon of mass $m_\oplus$) and by the thrust due to the E-sail propulsion system. Assuming a circular Earth+Moon orbit around the Sun, the spacecraft motion can be conveniently described within a synodic (rotating) reference frame $\mathcal{T}(C;x,y,z)$, having its origin at the system's center-of-mass C, with unit vectors $\hat{\mathbf{i}}$,$\hat{\mathbf{j}}$ and $\hat{\mathbf{k}}$, see Fig. 1.

Let G be the universal gravitational constant, $\mu\triangleq m_\oplus/(m_\oplus+m_\odot)\approx 3.0404\times10^{-6}$ the dimensionless mass of Earth+Moon, and $l\triangleq 1$ au the Sun–[Earth+Moon] distance (a constant value in the CRTBP). Let also $\boldsymbol{\rho}_\odot$,$\boldsymbol{\rho}_\oplus$, and $\mathbf{r}$ (with $\rho_\odot=\Vert\boldsymbol{\rho}_\odot\Vert$ and $\rho_\oplus=\Vert\boldsymbol{\rho}_\oplus\Vert$) be the spacecraft dimensionless position vectors, see Fig. 1. The

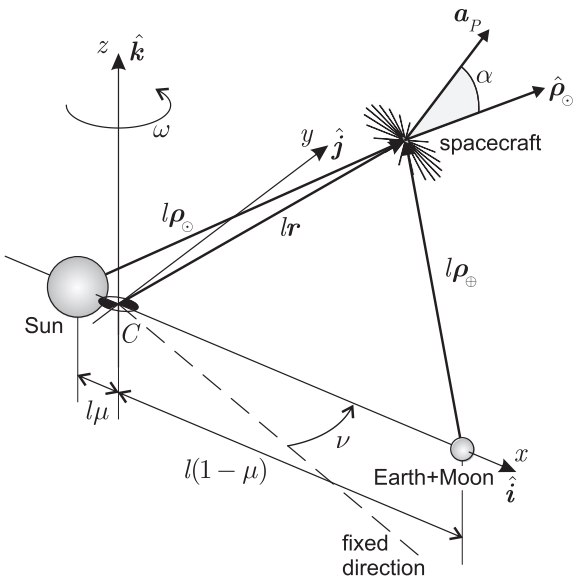

Fig. 1. Schematic of the Sun−[Earth+Moon] CRTBP with E-sail based spacecraft.

dimensionless spacecraft equations of motion in the synodic reference frame $\mathcal{T}$ are [19]

$$\boldsymbol{r}' = \boldsymbol{v} \tag{1}$$

$$\boldsymbol{v}' = \frac{l^2}{G(m_\odot + m_\oplus)}\boldsymbol{a}_P - \frac{1-\mu}{\rho_\odot^3}\boldsymbol{\rho}_\odot - \frac{\mu}{\rho_\oplus^3}\boldsymbol{\rho}_\oplus - \hat{\boldsymbol{k}} \times \left(\hat{\boldsymbol{k}} \times \boldsymbol{r}\right) - 2\,\hat{\boldsymbol{k}} \times \boldsymbol{v} \tag{2}$$

where the prime symbol denotes a derivative taken with respect to the angular variable $\nu \geq 0$ and

$$\boldsymbol{\rho}_\odot \triangleq \rho_\odot \hat{\boldsymbol{\rho}}_\odot = \boldsymbol{r} + \mu\hat{\boldsymbol{i}}, \boldsymbol{\rho}_\oplus \triangleq \rho_\oplus \hat{\boldsymbol{\rho}}_\oplus = \boldsymbol{r} - (1-\mu)\hat{\boldsymbol{i}} \tag{3}$$

Taking into account the recent plasmadynamic simulations [3] about the E-sail behaviour in the interplanetary space, the spacecraft propulsive acceleration in the CRTBP can be written as [11]

$$\boldsymbol{a}_P = \beta \frac{G\,m_\odot}{l^2\,\rho_\odot}\,\tau\,\hat{\boldsymbol{a}}_P \tag{4}$$

with $\hat{\boldsymbol{a}}_P \triangleq \boldsymbol{a}_P / \|\boldsymbol{a}_P\|$. The propulsive acceleration modulus is known to be inversely proportional to the Sun-spacecraft distance [20], that is, $\|\boldsymbol{a}_P\|$ varies proportional to $1/\rho_\odot$. Also, $\tau \in \{0,\ 1\}$ is a switching parameter that models the E-sail on/off condition and is introduced to account for coasting arcs in the spacecraft trajectory. Finally, β is the sail lightness number, defined as the ratio of the maximum propulsive acceleration modulus to the Sun's gravitational acceleration ($G\,m_\odot/l^2$) at the reference distance l. The sail lightness number β is a fundamental design parameter that quantifies the spacecraft's propulsive performance. It is closely related to the spacecraft characteristic acceleration a_c through the expression $a_c \triangleq \beta G m_\odot / l^2 \simeq 5.93\beta$, where a_c is given in millimeter per second squared. Recall that a_c is the maximum value of the propulsive acceleration modulus when the Sun-spacecraft distance is one astronomical unit.

As a consequence of the assumption that the celestial bodies cover circular orbits about their center of mass C, the time t turns out to be a linear function of ν, i.e. $\mathrm{d}\nu/\mathrm{d}t = \omega$, where the constant $\omega = 360/365.25$ deg/day coincides with the Earth's orbital angular velocity. In addition to the switching parameter, the second control variable is the thrust direction $\hat{\boldsymbol{a}}_P$. The angle between the Sun-sailcraft line and the thrust vector, referred to as sail cone angle α, cannot exceed a maximum value $\alpha_{\max}$, which is here set equal to $\alpha_{\max} \triangleq 30$ deg. From Fig. 1 the mathematical constraint, when the thrust is switched on, is therefore

$$\arccos(\hat{\boldsymbol{a}}_P \cdot \hat{\boldsymbol{\rho}}_\odot) \leq \alpha_{\max} \tag{5}$$

Note that the propulsive acceleration modulus is only dependent on the Sun-spacecraft distance. In other terms, the thrust of the sail is assumed to be independent of its direction within the allowable cone.

The problem addressed in this paper is to find the minimum-time spacecraft trajectory that transfers the spacecraft from a given initial state $\{\boldsymbol{r}_i,\ \boldsymbol{v}_i\}$ to a given final state $\{\boldsymbol{r}_f,\ \boldsymbol{v}_f\}$. The time histories of the two control variables τ and $\hat{\boldsymbol{a}}_P$ are hence obtained by solving an optimal control problem.

Assume, without loss of generality, that the initial angular position be $\nu_i \triangleq \nu(t_i) = 0$. Since the time varies linearly with ν, the minimum-time problem consists of minimizing the angular position $\nu_f \triangleq \nu(t_f)$, where t_f is the time at the end of the transfer. This amounts to finding the trajectory that maximizes the performance index $J \triangleq -\nu_f$. The optimal trajectory is sought using the dimensionless equations of motion (1)–(2), in which ν is the independent variable. Using an indirect approach, the minimum-time problem can be solved by maximizing the Hamiltonian

$$\mathcal{H} = \boldsymbol{\lambda}_r \cdot \boldsymbol{r}' + \boldsymbol{\lambda}_v \cdot \boldsymbol{v}' \tag{6}$$

where $\boldsymbol{\lambda}_r$ and $\boldsymbol{\lambda}_v$ are the vectors adjoint to $\boldsymbol{r}$ and $\boldsymbol{v}$, respectively. The time-derivatives of $\boldsymbol{\lambda}_r$ and $\boldsymbol{\lambda}_v$ are given by the Euler–Lagrange equations that, taking into account Eqs. (3) and (6), assume the compact form

$$\boldsymbol{\lambda}_r' \triangleq -\frac{\partial \mathcal{H}}{\partial \boldsymbol{r}} = \left[\frac{(1-\mu)}{\rho_\odot^3}(\mathbb{I} - 3\,\hat{\boldsymbol{\rho}}_\odot\,\hat{\boldsymbol{\rho}}_\odot) + \frac{\mu}{\rho_\oplus^3}(\mathbb{I} - 3\,\hat{\boldsymbol{\rho}}_\oplus\,\hat{\boldsymbol{\rho}}_\oplus) + \beta\,\tau\frac{(1-\mu)}{\rho_\odot^2}\hat{\boldsymbol{\rho}}_\odot\,\hat{\boldsymbol{a}}_P + \mathbb{E}^2\right] \cdot \boldsymbol{\lambda}_v \tag{7}$$

$$\boldsymbol{\lambda}_v' \triangleq -\frac{\partial \mathcal{H}}{\partial \boldsymbol{v}} = -\boldsymbol{\lambda}_r - 2\,\mathbb{E} \cdot \boldsymbol{\lambda}_v \tag{8}$$

where $\mathbb{I}$ is the 3×3 identity matrix and

$$\mathbb{E} \triangleq \begin{bmatrix} 0 & -1 & 0 \\ 1 & 0 & 0 \\ 0 & 0 & 0 \end{bmatrix} \tag{9}$$

From Pontryagin's maximum principle, the optimal control law maximizes, for any value of ν, a reduced Hamiltonian $\tilde{\mathcal{H}}$, corresponding to the portion of $\mathcal{H}$ that explicitly depends on the controls τ and $\hat{\boldsymbol{a}}_P$. Taking into account Eq. (4), the reduced Hamiltonian is

$$\tilde{\mathcal{H}} = \tau\, \hat{\boldsymbol{a}}_{\mathrm{P}} \cdot \hat{\boldsymbol{\lambda}}_v \tag{10}$$

Let $\theta \in [0,\ \pi]$ rad be the primer vector orientation angle, i.e. the angle between the direction of the primer vector $\boldsymbol{\lambda}_v$ and the direction of the Sun-spacecraft position vector $\boldsymbol{\rho}_{\odot}$, viz.

$$\theta = \arccos\left(\hat{\boldsymbol{\rho}}_{\odot} \cdot \hat{\boldsymbol{\lambda}}_v\right) \tag{11}$$

Eq. (10) states that the optimal propulsive thrust direction is such to maximize the admissible projection of $\boldsymbol{a}_{\mathrm{P}}$ along $\boldsymbol{\lambda}_v$. As a result, recalling the constraint (5), if $\theta \le \alpha_{\max}$ the thrust must be switched on ($\tau = 1$) and the propulsive acceleration is aligned along $\boldsymbol{\lambda}_v$, that is, $\hat{\boldsymbol{a}}_{\mathrm{P}} = \hat{\boldsymbol{\lambda}}_v$. If, instead, $\theta > (\alpha_{\max} + \pi/2)$, the thrust must be off ($\tau = 0$) otherwise $\tilde{\mathcal{H}}$ would be negative. Finally, if $\theta \in (\alpha_{\max}\ ,\ \alpha_{\max} + \pi/2]$, the thrust is on ($\tau = 1$), the cone angle is at its maximum ($\alpha = \alpha_{\max}$), the three unit vectors $\hat{\boldsymbol{a}}_{\mathrm{P}}$, $\hat{\boldsymbol{\lambda}}_v$ and $\hat{\boldsymbol{\rho}}_{\odot}$ are coplanar, and the thrust direction is between the directions of $\hat{\boldsymbol{\lambda}}_v$ and $\hat{\boldsymbol{\rho}}_{\odot}$. To summarize, the optimal control law is

$$\tau = \begin{cases} 0 & \text{if } \theta > \alpha_{\max} + \pi/2 \\ 1 & \text{if } \theta \le \alpha_{\max} + \pi/2 \end{cases} \tag{12}$$

$$\hat{\boldsymbol{a}}_{\mathrm{P}} = \begin{cases} \hat{\boldsymbol{\lambda}}_v & \text{if} \quad \theta \le \alpha_{\max} \\ \dfrac{\sin(\theta - \alpha_{\max})}{\sin\theta}\hat{\boldsymbol{\rho}}_{\odot} + \dfrac{\sin\alpha_{\max}}{\sin\theta}\hat{\boldsymbol{\lambda}}_v & \text{if} \quad \theta \in (\alpha_{\max}, \alpha_{\max} + \pi/2] \end{cases} \tag{13}$$

The differential system is constituted by the equations of motion Eqs. (1)–(2), and by the Euler–Lagrange equations (7)–(8), whose control laws are given by Eqs. (12) and (13). The differential system is completed by twelve scalar boundary conditions, corresponding to the six components of the initial state vector $\{\boldsymbol{r}_i,\ \boldsymbol{v}_i\}$ and the six components of the final state vector $\{\boldsymbol{r}_f,\ \boldsymbol{v}_f\}$. The trasversality condition [21], $\mathcal{H}(\nu_f) = 1$, is used to find the minimum value of ν_f.

The transfer analysis is much simplified for a two-dimensional problem, corresponding, for example, to a situation in which the transfer trajectories are in the ecliptic plane, or in the plane (x,y) of the synodic reference frame. This is the simplified mission scenario adopted in the succeeding analysis. Its practical importance will be discussed in the next section. Note that the resulting trajectories, albeit two-dimensional, have been validated using the full (three-dimensional) model of the spacecraft dynamics.

3. Mission applications

The previous minimum-time problem has been adopted to investigate two different mission applications involving the transfer trajectory of an E-sail spacecraft between two equilibrium points. In all of the numerical simulations the differential equations have been integrated in double precision using a variable order Adams–Bashforth–Moulton solver scheme [22,23] with absolute and relative errors of 10^{-12}. The TPBVP associated to the optimization process has been solved, with an absolute error less than 10^{-8}, through a hybrid numerical technique that combines genetic algorithms to obtain a first estimate of the four adjoint variables unknown, with gradient-based and direct methods to refine the solution.

It is worth noting that solving the TPBVP can only guarantee that the first order necessary conditions for the optimization are satisfied. For that reason a suitable procedure has been adopted to reduce the possibility of the solution converging to a local maximum. In particular, for each mission scenario the TPBVP has been solved starting from different initial guess solutions. The "candidate" optimal value is chosen to correspond to the maximum value of the performance index J within the set of the results obtained. The solution thus obtained is then perturbed by slightly varying the unknown variables. The TPBVP is solved again to check whether the new solution still converges to the same performance index. Although the above procedure does not guarantee the global optimality of the solution, it has been successfully used by the authors in a number of different mission scenarios. The following results can therefore be considered as minimum time solutions at least in the spirit of a preliminary mission analysis.

3.1. Geostorm mission scenario

The first case discussed is inspired by the Geostorm Warning Mission [13,24], now the Heliostorm mission [25], whose aim is to provide an early warning of possible geomagnetic storms. The fundamental mission requirement is to transfer a spacecraft at a collinear (closer to the Sun) AEP of the Sun–Earth system, whose distance from the planet is twice as much as the distance of the natural Lagrangian point L_1. Such an AEP location, referred to as P_{gs}, must then be maintained for a prolonged mission time by means of a suitable propulsion system. For example, the operating time requirement for the Geostorm mission was between 3 and 5 years [13]. The only way to guarantee such a time requirement is to use a propellantless thruster. The original mission was indeed conceived for a solar sail spacecraft [26], but the same mission scenario has been recently revisited [27] to quantify the performance of an E-sail, with particular attention to the generation of halo orbits around the AEP.

In this case, the problem is to investigate the minimum-time trajectories between L_1 and P_{gs} for an E-sail based spacecraft. This situation is consistent, for example, with that discussed in Ref. [16], in which a spacecraft equipped with a propellantless propulsion system is initially parked at L_1, and is then transferred to another AEP to accomplish the mission. The positions of the two points in the synodic frame are $[\boldsymbol{r}_{L_1}]_{\mathcal{T}} = [x_{L_1}/l,\ 0,\ 0]^{\mathrm{T}}$, and $[\boldsymbol{r}_{\mathrm{gs}}]_{\mathcal{T}} = [(2x_{L_1}/l + \mu - 1),\ 0,\ 0]^{\mathrm{T}}$, where $x_{L_1}/l = 0.99$.

The lightness number used in the simulations is $\beta \simeq 0.0526$, corresponding to a characteristic acceleration of about $a_c \simeq 0.3122\ \mathrm{mm/s^2}$. The latter is the value required to maintain a spacecraft at P_{gs}, as it can be verified through the results taken from Ref. [11]. Using the boundary conditions $\boldsymbol{r}_i = \boldsymbol{r}_{L_1}$, $\boldsymbol{r}_f = \boldsymbol{r}_{\mathrm{gs}}$, and $\boldsymbol{v}_i = \boldsymbol{v}_f = 0$, the solution of the TPBVP provides the optimal trajectory drawn in Fig. 2. This trajectory all belongs to the ecliptic plane.

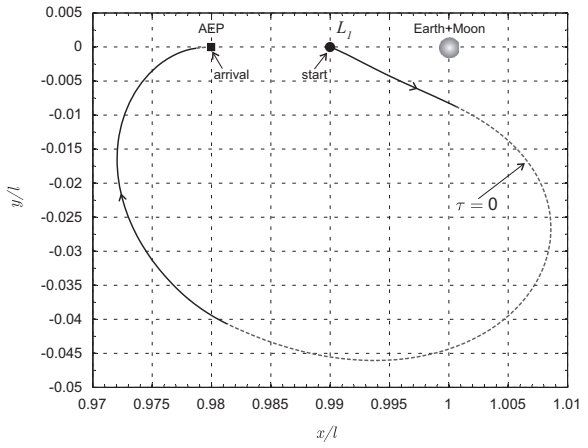

Fig. 2. Optimal transfer trajectory in the Geostorm scenario (solid line: $\tau = 1$, dashed line: $\tau = 0$).

The optimal angle swept by the Earth+Moon during the spacecraft displacement is $\nu_f = 250.6$ deg, which corresponds to a minimum flight-time of about 254 days. The dimensionless components of the spacecraft position and velocity vectors are shown in Fig. 3 as a function of the angular position. A significant portion of the optimal trajectory, longer than one half of the total transfer time, is flown with the thruster switched off ($\tau = 0$). In particular, Fig. 3 emphasizes the presence of two coasting arcs. The second arc is engaged shortly before the conclusion of the mission, which, indeed, ends with a coasting phase. Note, however, that the E-sail must be switched on again as soon as the spacecraft reaches the target AEP, where the spacecraft thrust must be aligned along the Sun–[Earth-+Moon] direction to meet the equilibrium conditions and maintain the AEP location [11].

3.2. Motion between Lagrangian points

The second mission scenario involves the transfer between a subset of the classical Lagrangian points [15]. The coordinates of the points involved in the problem, L_1, L_3, L_4, and L_5, are summarized in Table 1. The fifth classical Lagrangian point, L_2, has not been considered in this study because the effectiveness of the propulsion system around that point could be much affected by the solar wind interaction with Earth's magnetosphere.

The minimum-time transfer trajectory between each pair of AEPs in Table 1 has been calculated assuming a spacecraft characteristic acceleration $a_c = 1$ mm/s^2, corresponding to a sail lightness number $\beta \simeq 0.1686$. In all of the simulations, the initial and final (relative) velocities in the synodic frame were set equal to zero, i.e. $\boldsymbol{v}_i \equiv \boldsymbol{v}_f = 0$. Such a choice models a situation in which the spacecraft maintains the AEP position for a suitable time interval, whose length is, however, not included in the optimization process, but it is related to other mission constraints. The minimum flight times for the 12 optimal transfer trajectories have been summarized in Table 2.

It is worth noting that the symmetry in the transfer times is highlighted in some entries of Table 2. For example, the transfer time from L_4 to L_1 is the same as the time from L_1 to L_5. Likewise, the transfer time between L_5 and L_3 equals that from L_4 and L_5. These symmetries arise from the fact that Eqs. (1)–(4) are invariant under the transformation $(\boldsymbol{r}, \boldsymbol{r}', \tau, \hat{\boldsymbol{a}}_P, t) \rightarrow (\mathbb{T}\boldsymbol{r}, -\mathbb{T}\boldsymbol{r}', \tau, \mathbb{T}\hat{\boldsymbol{a}}_P, -t)$, where $\mathbb{T} \triangleq \mathrm{diag}(1, -1, 1)$. Such a transformation extends a similar result that applies to trajectories in the CRTBP [28] in the ballistic case (i.e., when $\beta = 0$, or the propulsion system is always switched-off). Note that the existence of these symmetries reduces the possibility that the solution of the TPBVP associated to the optimum problem may

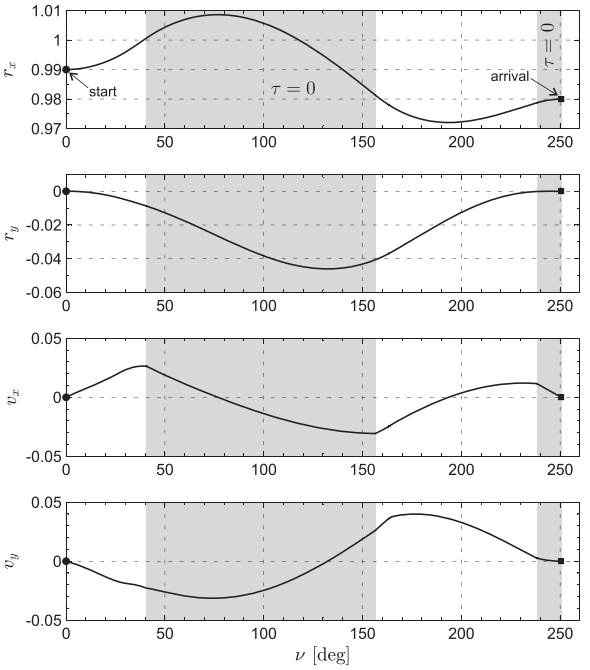

Fig. 3. Optimal transfer in the Geostorm scenario: components of $\boldsymbol{r}$ and $\boldsymbol{v}$ as a function of ν.

Table 1
Position, in the (x,y) plane, of the classical Lagrangian points.

Lagran. point	Position		
	x/l	y/l	z/l
L_1	0.99	0	0
L_3	−1	0	0
L_4	0.5	0.866	0
L_5	0.5	−0.866	0

Table 2
Optimal flight times, in days, between pairs of Lagrangian points ($a_c = 1$ mm/s^2).

Starting point	Final point			
	L_1	L_3	L_4	L_5
L_1	–	475	445	287
L_3	475	–	390	553
L_4	287	553	–	390
L_5	445	390	553	–

converge to a local maximum of the performance index J. In fact, the symmetry condition represents a further means to compare different solutions and exclude possible sub-optimal trajectories. Such an expedient has been successfully used to avoid the convergence toward local maxima, a problem that has been experienced especially in the transfers between L_4 and L_3.

The same symmetry existing in the transfer times is also apparent in the spacecraft optimal trajectories between Lagrangian points drawn in Fig. 4. For the sake of clearness the figure is divided in two parts according to whether the generic trajectory involves the point L_3 (see Fig. 4(a)) or not (see Fig. 4(b)). The coasting phases are illustrated with dashed lines and the arrows point out the direction of motion. Unlike the case discussed in the previous section, in this example the mission starts and ends with a propelled arc. However, when the generic Lagrangian point is reached, the spacecraft thrust must be switched-off to maintain the relative equilibrium position.

From the data of Table 2, and using the sequence $L_1 \rightarrow L_5 \rightarrow L_3 \rightarrow L_4 \rightarrow L_1$, an E-sail based spacecraft with a

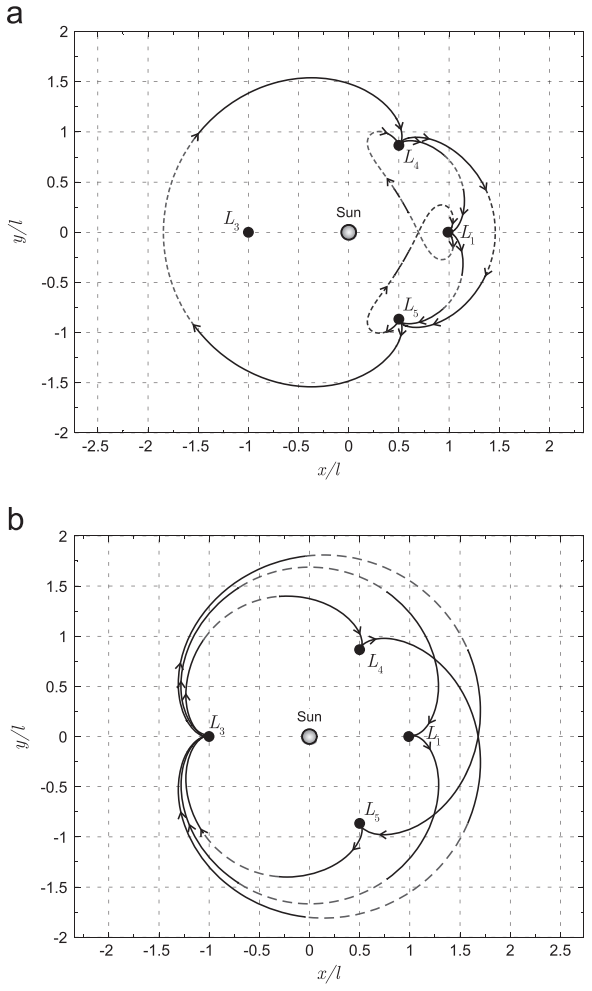

Fig. 4. Optimal transfer trajectories between Lagrangian points when $a_c = 1$ mm/s^2 (solid line: $\tau = 1$, dashed line: $\tau = 0$). (a) Trajectories without L_3. (b) Trajectories towards/from L_3.

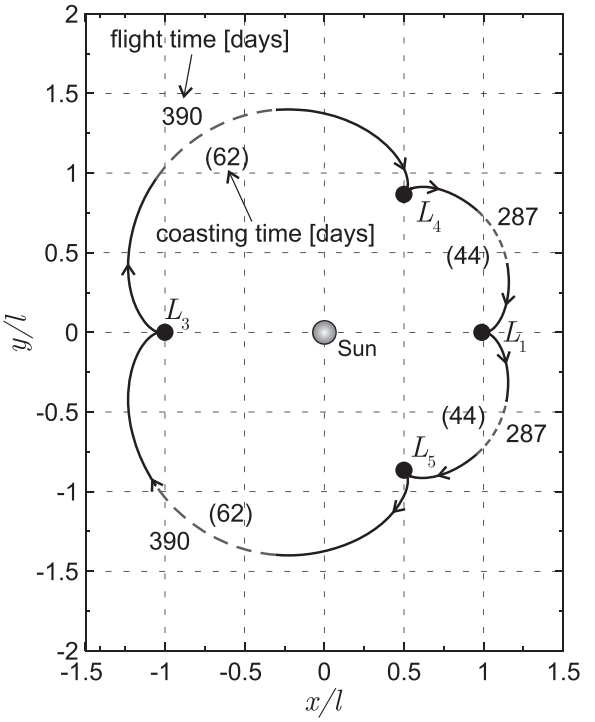

Fig. 5. Optimal tour of the Lagrangian points when $a_c = 1$ mm/s^2 (solid line: $\tau = 1$, dashed line: $\tau = 0$).

characteristic acceleration of 1 mm/s^2 may complete a tour of the four Lagrangian points within a total flight time of 1354 days (about 3.71 years). The corresponding optimal trajectory tracked by the spacecraft is illustrated in Fig. 5, which also shows the length of the various coasting phases. The sum of all coasting times amounts to about 16%, thus confirming the crucial contribution of the propulsion system for obtaining the minimum time trajectory. The flight parameters thus obtained represent a fundamental starting point for a succeeding mission analysis, including the effects of the solar wind variation on the capability of maintaining a given AEP, and for a further refinement of the transfer performance evaluation.

4. Conclusions

Minimum time trajectories for an electric solar wind sail have been studied within the circular restricted three body problem constituted by the Sun and the Earth+Moon. The problem has been addressed using a variational approach and has been applied to two different mission scenarios. An Electric Solar Wind Sail of modest performance is sufficient for reaching and maintaining a collinear artificial equilibrium point located at a distance from the Earth twice as much as the distance of the classical point L_1. The minimum transfer time necessary to reach the artificial collinear equilibrium point is about 250 days.

As a second example, a complete tour of a subset of the classical Lagrangian points has been shown to be feasible in less than four years, using a spacecraft with a characteristic acceleration of 1 mm/s^2. The transfer trajectories

confirm interesting symmetries that arise from the structure of the equation of motion. The presence of those symmetries in the transfer trajectories, which has been demonstrated in an analytic form, represents an original contribution of the paper. This results extends a similar well-known property of ballistic transfers within the Circular Restricted Three Body Problem. The simulation data can be used as a starting point for a more accurate mission analysis that should take into account the actual eccentricities of the planetary orbits and the significant thrust reduction associated to a spacecraft entry into the Earth's magnetosphere. A natural extension of this work could take into account the effects of a change in the sail performance parameter, for example a time variation in the sail voltage, which induces a change in the characteristic acceleration during the transfer. Indeed, more flexibility in the trajectory design can be obtained by considering the characteristic acceleration as an additional control means.

References

[1] P. Janhunen, A. Sandroos, Simulation study of solar wind push on a charged wire: basis of solar wind electric sail propulsion, Ann. Geophys. 25 (3) (2007) 755–767.

[2] P. Janhunen, Electric sail for spacecraft propulsion, J. Propuls. Power 20 (4) (2004) 763–764, http://dx.doi.org/10.2514/1.8580.

[3] P. Janhunen, et al., Electric solar wind sail: toward test missions, Rev. Sci. Instrum. 81 (11) (2010) 111301–111311, http://dx.doi.org/10.1063/1.3514548.

[4] P. Janhunen, et al., Overview of electric solar wind sail applications, Proc. Est. Acad. Sci. 63 (2S) (2014) 267–278, http://dx.doi.org/10.3176/proc.2014.2S.08.

[5] V. Szebehely, Theory of Orbits: The Restricted Problem of Three Bodies, Academic Press, New York, 1967 ISBN: 0126806500.

[6] C. Circi, Properties of transit trajectory in the restricted three and four-body problem, Adv. Space Res. 49 (10) (2012) 1506–1519, http://dx.doi.org/10.1016/j.asr.2012.02.034.

[7] D. Romagnoli, C. Circi, Earth-moon weak stability boundaries in the restricted three and four body problem, Celest. Mech. Dyn. Astron. 103 (1) (2009) 79–103, http://dx.doi.org/10.1007/s10569-008-9169-y.

[8] C. Circi, P. Teofilatto, Effect of planetary eccentricity on ballistic capture in the solar system, Celest. Mech. Dyn. Astron. 93 (1–4) (2005) 69–86, http://dx.doi.org/10.1007/s10569-005-3640-9.

[9] C.R. McInnes, A.J.C. McDonald, J.F.L. Simmons, E.W. MacDonald, Solar sail parking in restricted three-body systems, J. Guid. Control Dyn. 17 (2) (1994) 399–406, http://dx.doi.org/10.2514/3.21211.

[10] G. Aliasi, G. Mengali, A.A. Quarta, Artificial equilibrium points for a generalized sail in a circular restricted three-body problem, Celest. Mech. Dyn. Astron. 110 (4) (2011) 343–368, http://dx.doi.org/10.1007/s10569-011-9366-y.

[11] G. Aliasi, G. Mengali, A.A. Quarta, Artificial equilibrium points for electric sail with constant attitude, J. Guid. Control Dyn. 50 (6) (2013) 1295–1297, http://dx.doi.org/10.2514/1.A32540.

[12] M. Morimoto, H. Yamakawa, K. Uesugi, Artificial equilibrium points in the low-thrust restricted three-body problem, J. Guid. Control Dyn. 30 (5) (2007) 1563–1567, http://dx.doi.org/10.2514/1.26771.

[13] J.L. West, The geostorm warning mission: enhanced opportunities based on new technology, in: 14th AAS/AIAA Space Flight Mechanics Conference, Maui, HI, 2004, paper AAS 04-102.

[14] C.G. Sauer, Jr., The L1 diamond affair, in: 14th AAS/AIAA Space Flight Mechanics Conference, Maui, HI, 2004, paper AAS 04-278.

[15] A. Farrés, A. Jorba, Solar sail surfing along families of equilibrium points, Acta Astronaut. 63 (1–4) (2008) 249–257, http://dx.doi.org/10.1016/j.actaastro.2007.12.021.

[16] J. Heiligers, C.R. McInnes, Agile solar sailing in three-body problem: motion between artificial equilibrium points, in: 64th International Astronautical Congress, Bejing, China, 2013, paper IAC-13-C1.8.3.

[17] E. Kulu, et al., Estcube-1 nanosatellite for electric solar wind sail demonstration in low earth orbit, in: Proceedings of the 64th International Astronautical Congress, vol. 5, Beijing, China, 2013, pp. 3898–3902.

[18] J. Envall, et al., E-sail test payload of the estcube-1 nanosatellite, Proc. Est. Acad. Sci. 63 (2S) (2014) 210–221, http://dx.doi.org/10.3176/proc.2014.2S.02.

[19] R.H. Battin, An Introduction to the Mathematics and Methods of Astrodynamics, AIAA, New York, 1987, pp. 371–382, ISBN: 1-563-47342-9.

[20] P. Janhunen, The electric solar wind sail status report, in: European Planetary Science Congress 2010, vol. 5, Rome, Italy, 2010, paper EPSC 2010-297.

[21] A.E. Bryson, Y.C. Ho, Applied Optimal Control, Hemisphere Publishing Corporation, New York, NY, 1975, Ch. 2, pp. 71–89, ISBN: 0-891-16228-3.

[22] L.F. Shampine, M.K. Gordon, Computer Solution of Ordinary Differential Equations: The Initial Value Problem, W.H. Freeman & Co Ltd, San Francisco, 1975, Ch. 10, ISBN: 0-716-70461-7.

[23] L.F. Shampine, M.W. Reichelt, The MATLAB ODE suite, SIAM J. Sci. Comput. 18 (1) (1997) 1–22, http://dx.doi.org/10.1137/S1064827594276424.

[24] C.W.L. Yen, Solar sail geostorm warning mission design, in: 14th AAS/AIAA Space Flight Mechanics Conference, Maui, HI, 2004, paper AAS 04-107.

[25] R. Young, Updated heliostorm warning mission: enhancements based on new technology, in: 48th AIAA/ASME/ASCE/AHS/ASC Structures, Structural Dynamics, and Materials Conference, Honolulu, HI, 2007, paper AIAA 2007-2249.

[26] C.R. McInnes, Solar sailing: technology, dynamics and mission applications, Springer-Praxis Series in Space Science and Technology, Springer-Verlag, 1999, pp. 38–40, 231–238, 250–256, ISBN: 1-852-33102-X.

[27] G. Aliasi, G. Mengali, A.A. Quarta, Artificial periodic orbits around L_1-type equilibrium points for a generalized sail, J. Guid. Control Dyn., 2015, in press. http://dx.doi.org/10.2514/1.G000904.

[28] E.J. Doedel, V.A. Romanov, R.C. Paffenroth, H.B. Keller, D.J. Dichmann, J. Galán-Vioque, A. Vanderbauwhede, Elemental periodic orbits associated with the libration points in the circular restricted 3-body problem, Int. J. Bifurc. Chaos 17 (8) (2007) 2625–2677, http://dx.doi.org/10.1142/S0218127407018671.

All in-text references underlined in blue are linked to publications on ResearchGate, letting you access and read them immediately.